International Journal of Thermophysics (2021) 42:12
https://doi.org/10.1007/s10765-020-02757-x

Heat Transfer Capability of Ionanofluids for Heat Transfer Applications

Gabriela Huminic[1] · **Angel Huminic**[1]

Received: 6 October 2020 / Accepted: 16 October 2020 / Published online: 11 November 2020

Abstract

Ionanofluids are mixtures of ionic liquid and solid particles with enhanced thermophysical properties. Using the properties of these ionanofluids (thermal conductivity, dynamic viscosity, specific heat, and density), a comprehensive analysis concerning their heat transfer capability was performed. Two nanomaterials, silicon carbide (SiC) and graphene dispersed in 1-hexyl-3-methylimidazolium tetrafluoroborate ([H_{mim}]SF_4) were studied. Different equations (figures of merit) as a base of comparison for laminar and turbulent flows were used. The effects of concentration and temperature on the pumping power ratio were theoretically investigated. The results indicated that the studied ionanofluids can contribute to the enhancement of thermal performance, especially in laminar flow.

Keywords Efficiency · Ionanofluid · Pumping power

Nomenclature

Variables

c_p	Specific heat, J·(kg·K)$^{-1}$
h	Heat transfer coefficient, W·(m^2·K)$^{-1}$
k	Thermal conductivity, W·(m·K)$^{-1}$
Mo	Mouromtseff number
W	Pumping power, W

Greek symbols

μ	Dynamic viscosity, Pas
ρ	Density, kg·m^{-3}

This article is part of the Special Issue on Nanoparticle-enhanced Ionic Liquids.

✉ Gabriela Huminic
gabi.p@unitbv.ro

[1] Mechanical Engineering Department, Transilvania University of Brasov, 29, Bulevardul Eroilor, 500036 Brasov, Romania

Subscript

INF	Ionanofluid
BF	Base fluid
L	Laminar
r	Ratio
T	Turbulent

Abbreviations

$[B_{MIM}][BF_4]$	f 1-Butyl-3-methylimidazolium tetrafluoroborate
$[C4_{mim}][NTf2]$	1-Butyl-3-methylimidazolium bis(trifluoromethylsulfonyl) imide
$[C4_{mpyrr}][NTf2]$	*N*-Butyl-*N*-methylpyrrolidiniumbis(trifluoromethanesulfonyl) imide
$[C2_{mim}][CH_3SO_3]$	1-Ethyl-3-methylimidazolium methanesulfonate
$[E_{MIm}]Ac)$	1-Ethyl-3-methylimidazolium acetate
$[E_{MIM}][DEP]$	1-Ethyl-3-methylimidazolium diethylphosphate
$[H_{mim}]BF_4$	1-Hexyl-3-methylimidazolium tetrafluoroborate
$[N_{4111}][NTf2]$	Butyltrimethylammoniumbis(trifluoromethylsulfonyl)imide
FOM	Figure-of-merit

1 Introduction

Ionanofluids are mixtures of ionic liquid and solid particles with enhanced thermophysical properties (thermal conductivity and heat capacity) which may be used as alternative fluids both to conventional fluids and nanofluids, in order to improve heat transfer in thermal systems. In the last years, ionanofluids were used as working fluids in various solar applications (solar thermal collectors, solar heating systems).

The first studies on ionanofluids were carried out by Ribeiro et al. [1]. Numerous studies afterward indicated and confirmed the significant features of these fluids. Thus, Zhang et al. [2] investigated the thermal conductivity, viscosity, heat specific capacity and heat transfer performance of the 1-ethyl-3-methylimidazolium acetate ([EMIm]Ac)–graphene nanoplatelets (GNPs) ionanofluid at various temperatures and mass fractions. They reported an increase in the thermal conductivity of 43.2 % that corresponds to an increase in the heat transfer coefficient of 28.6 %.

Paul et al. [3] studied the thermal conductivity, heat capacity and the rheological behavior of $[C4_{mim}][NTf2]$, $[C4_{mmim}][NTf2]$, $[C4_{mpyrr}][NTf2]$, and $[N_{4111}][NTf2]$ with alumina nanoparticles and found an increase in thermal conductivity with increasing nanoparticles concentration up to 11 %, an average increase in heat capacity up to 62 % and also a significant increase in viscosity with increasing concentration. The results indicated a shear thinning behavior for all studied ionanofluids.

Thermal conductivity, density and viscosity of the f 1-butyl-3-methylimidazolium tetrafluoroborate $[B_{MIM}][BF_4]$ and nanodiamond (ND) ionanofluid were measured by Jorjani et al. [4]. Their results showed a maximum increase in thermal conductivity and viscosity up to 9.3 % and 126 % at a temperature of 25 °C and a volume concentration of 1.04 %. Also, they noticed a non-Newtonian behavior of ionanofluid. Concerning the density of studied ionanofluid, this property increases with increasing concentration and decreases with increasing temperature.

Relevant studies in the ionanofluids field were carried out by Minea and co-workers [5–8]. The results on rheological behavior and isobaric specific heat capacity of the mixture of 1-ethyl-3-methylimidazolium methanesulfonate $[C2_{mim}][CH_3SO_3]$ (0.75) + water (0.25) and alumina nanoparticles were presented in Ref. [5]. In this study, they noticed two types of behavior of the studied ionanofluid: a Newtonian behavior at low nanoparticles concentrations and a non-Newtonian behavior if the concentration is increased (for 3.38 % and 5.28 % vol. Al_2O_3). Also, the results indicated a maximum increase in viscosity up to 78 %, while the maximum decrease in isobaric specific heat capacity was 9.9 %. By comparing experimental results with theoretical models, they concluded that neither theoretical model cannot be used to predict the increase in viscosity with increasing concentration.

In another study, Minea et al. [6] performed a numerical study on the behavior of $[C2_{mim}][CH_3SO_3]$ (0.75) + water (0.25) and alumina nanoparticles mixture, $[C2_{mim}]$[CH3SO3] + water mixture and water in laminar convective flow. They found that by adding water to the ionic liquid ($[C2_{mim}][CH_3SO_3]$), the convective heat transfer coefficient decreases up to 70 %. By reporting the results for the heat transfer coefficient to those for pumping power, they concluded that ionanofluid with 5 %–10 % wt. Al_2O_3 can be a good alternative to ionic liquid for thermal applications. In another article, Cherecheş and Minea [7] investigated the electrical conductivity of ionanofluids based on water–$[C2_{mim}][CH_3SO_3]$ ionic liquids and alumina nanoparticles mixtures and found that by adding nanoparticles to the water–$[C2_{mim}][CH_3SO_3]$ mixture, the electrical conductivity decreases up to 60 %.

Effects of temperature, nanoparticles concentration and mass mole of water on thermal conductivity, viscosity and density of 1-ethyl-3-methylimidazolium diethylphosphate $[E_{MIM}]$[DEP], or its aqueous solution$[E_{MIM}]$[DEP] + water and MWCNTs were investigated by Zhao et al. [8]. Their results showed that all properties of ionanofluids are improved if MWCNTs are added to their base fluid.

Thermo-physical and radiative properties, as well as photo-thermal conversion performance of the $[B_{MIM}]BF_4$ ionic liquid with GNPs, SWCNTs, and GE materials were investigated by Zhang et al. [9]. The results showed that the $[B_{MIM}]BF_4$ + GE exhibit the highest thermal conductivity ratios compared to the GNPs- and SWCNTs at the same mass fractions and also that the viscosity of $[B_{MIM}]BF_4$ + GE decreases with increasing mass fraction, while the viscosity of GNPs- and SWCNTs showed the similar trend (decrease followed by an increase with increasing concentration).

Extensive reviews on ionic liquids and ionanofluids were published by Minea [10], Minea and Murshed [11], Wegner and Janiak [12] and Habib et al. [13].

In the current study, two types of ionanofluids, $[H_{mim}]BF_4$ + SiC and $[H_{mim}]BF_4$ + graphene, having the same base fluid, different nanomaterials, and the same weight concentrations will be discussed in terms of heat transfer efficiency. The reason for choosing the two ionanofluids for the study is the different variation of the properties (viscosity and density) with increasing concentration.

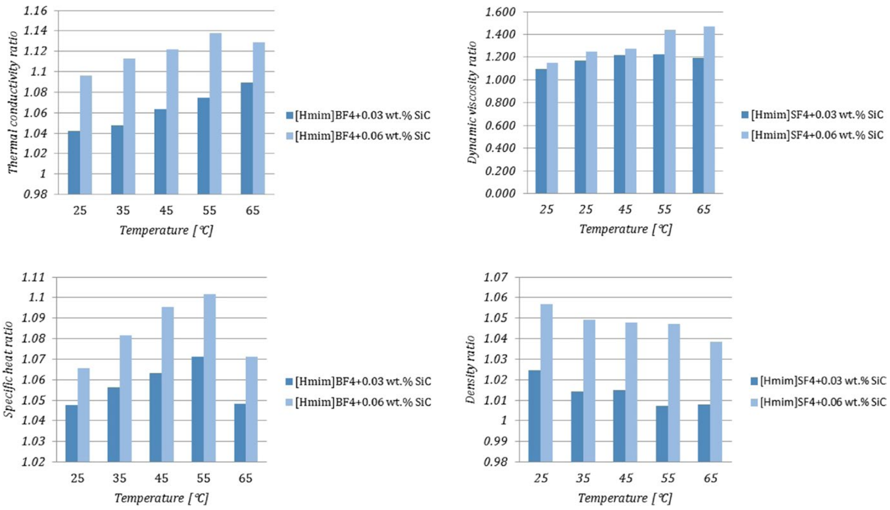

Fig. 1 The variation of the relative thermo-physical properties with concentration and temperature—$[H_{mim}]$SF4 + SiC ionanofluid

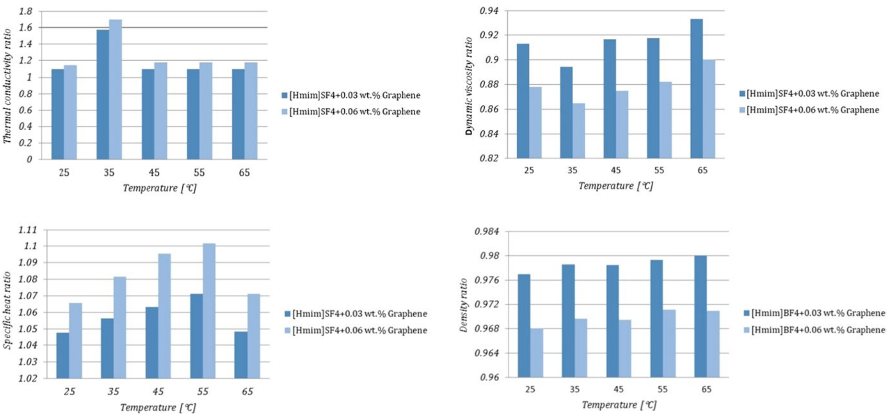

Fig. 2 The variation of the relative thermo-physical properties with concentration and temperature—$[H_{mim}]$SF4 + graphene ionanofluid

2 Thermo-physical Properties of Ionanofluids

The thermo-physical properties of the two types of ionanofluids used for this study were adopted from Zou [14] and Zhang [15]. Figures 1 and 2 depict the results on relative thermo-physical properties of $[H_{mim}]SF_4$ + SiC and $[H_{mim}]SF_4$ + graphene, computed with Eqs. 1–4:

$$\text{Thermal conductivity ratio}: k_r = \frac{k_{INF}}{k_{BF}}, \tag{1}$$

$$\text{Dynamic viscosity ratio}: \mu_r = \frac{\mu_{INF}}{\mu_{BF}}, \tag{2}$$

$$\text{Specific heat ratio}: c_{p,r} = \frac{c_{p,INF}}{c_{p,BF}}, \tag{3}$$

$$\text{Density ratio}: \rho_r = \frac{\rho_{INF}}{\rho_{BF}}. \tag{4}$$

3 Results and Discussion

3.1 Heat Transfer Efficiency of Ionanofluids

In current study, two types of ionanofluids, $\left[H_{mim}\right]BF_4 + SiC$ and $\left[H_{mim}\right]BF_4 + graphene$, with different weight concentrations (0.03 % and 0.06 %) and temperatures (25 °C–65 °C) will be discussed from point of view of heat transfer efficiency and their benefits compared to the base fluid ($\left[H_{mim}\right]BF_4$).

The Mouromtseff number used to evaluate of performance of ionanofluids in various heat transfer applications was present for the first time by Simons [16]. This number is based on one or more characteristics of fluids (thermal conductivity, dynamic viscosity, specific heat and density) and in general form is defined as:

$$Mo = \frac{k^a \rho^b c_p^c}{\mu^d}, \tag{5}$$

where the exponents a, b, c, and d take on values appropriate to the heat transfer mode of interest and the corresponding heat transfer correlation.

3.1.1 Efficiency of Ionanofluids in Internal Laminar Flows

An equation known for evaluating the efficiency of ionanofluids in laminar flow is based on the ratio between dynamic viscosity and thermal conductivity [17]:

$$\frac{C_\mu}{C_k} = \frac{\left(\mu_{INF} - \mu_{BF}\right)/\mu_{BF}}{\left(k_{INF} - k_{BF}\right)/k_{BF}}. \tag{6}$$

If this ratio is less than 4, it is considered that the ionanofluids are efficient compared to the base fluid.

Figure 3a, b illustrates the efficiency of all studied ionanofluids at various temperatures and weight concentrations of nanoparticles. One can notice that the both studied ionanofluids have values of ratio C_μ/C_k lower than 4 for all temperatures and nanoparticles concentrations. Moreover, the results indicated that $[H_{mim}]SF_4$ + graphene ionanofluid has the values of ratio C_μ/C_k much lower than

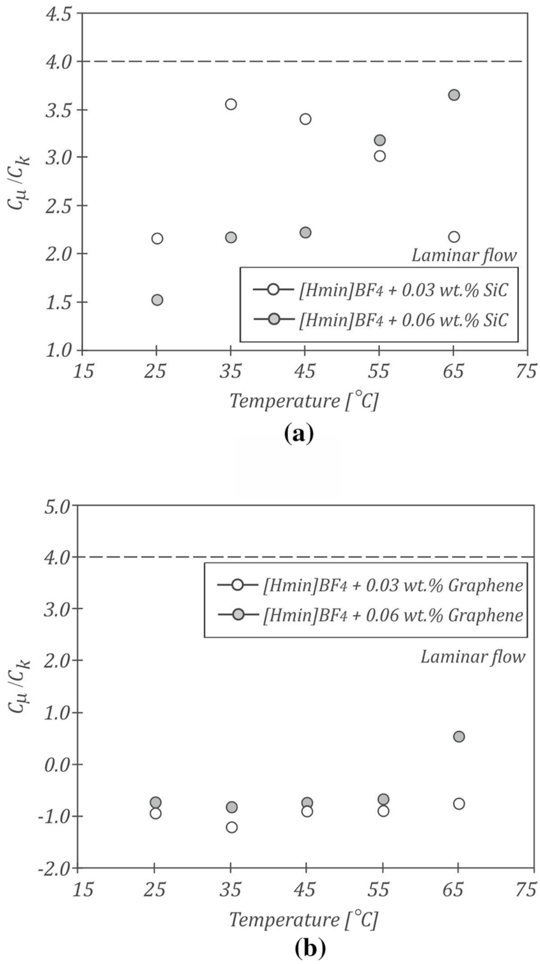

Fig. 3 Heat transfer efficiency based on Eq. 6

$[H_{mim}]SF_4 + SiC$ ionanofluid. This is due to dynamic viscosity of those two ionanofluids: for $[H_{mim}]SF_4 + SiC$ ionanofluid, the viscosity increases with increasing nanoparticles concentration, while for $[H_{mim}]SF_4$ + graphene ionanofluid the viscosity decreases with increasing concentration. Thus, it can be concluded that both ionanofluids have a higher efficiency than that of the base fluid $[H_{mim}]SF_4$) in internal laminar flow.

Another indicator to evaluate of the efficiency of ionanofluids in fully developed internal laminar flows is based on the ratio between the thermal conductivities of ionanofluid and the base fluid [16]:

$$Mo = \frac{k_{INF}}{k_{BF}}. \tag{7}$$

Mouromtseff number higher than 1 (Mo > 1) indicates better heat transfer capability of ionanofluid.

Figure 4a, b shows the Mouromtseff number for the studied ionanofluid. As can be seen, the Mo number is higher than 1 for all the studied temperatures and nanoparticles concentrations. For $[H_{mim}]SF_4 + SiC$ ionanofluid, there is an increase in Mo number with increase in both temperature and concentration, while for $[H_{mim}]SF_4 +$ graphene ionanofluid it can be seen that the temperature does not significantly influence the values of Mo number. Also, it is noticed that the values of Mo number are higher for $[H_{mim}]SF_4 +$ graphene ionanofluid compared to $[H_{mim}]SF_4 + SiC$ ionanofluid, which indicates that the $[H_{mim}]SF_4 +$ graphene ionanofluid is more efficient than $[H_{mim}]SF_4 + SiC$ ionanofluid in laminar flow.

3.1.2 Efficiency of Ionanofluids in Internal Turbulent Flows

In the internal turbulent flow the efficiency of ionanofluid is based on the Mouromtseff number (Mo) written in the form [18]:

Fig. 4 Heat transfer efficiency based on Eq. 7

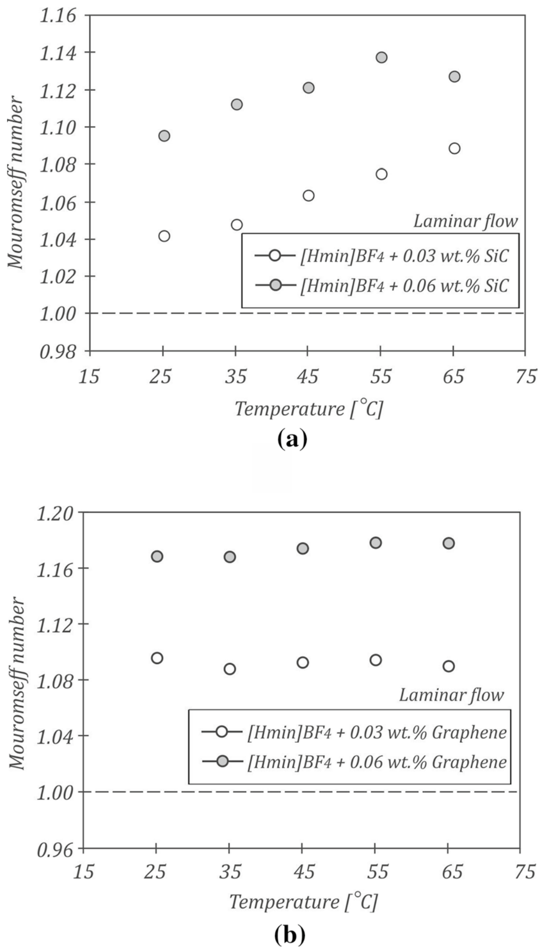

$$Mo = \frac{\frac{\rho_{INF}^{0.8} k_{INF}^{0.67} c_{p,INF}^{0.33}}{\mu_{INF}^{0.47}}}{\frac{\rho_{BF}^{0.8} k_{BF}^{0.67} c_{p,BF}^{0.33}}{\mu_{BF}^{0.47}}}. \tag{8}$$

In this case, if the Mo number is higher than 1, the ionanofluid could be considered as advantageous fluid for heat transfer applications.

Figure 5a, b depicts the heat transfer efficiency of studied ionanofluids with the variation of both temperature and concentration. In the case of $[H_{mim}]SF_4$ + SiC ionanofluid, it can be seen that only ionanofluid with a concentration of 0.06 % at temperatures up to 45 °C is beneficial for thermal applications, while for a concentration of 0.03 % this type of ionanofluis is not indicated regardless of operating temperature. Moreover, Fig. 5a shows a decrease in Mo number with increasing temperatures, the maximum values being obtained at 25 °C. For $[H_{mim}]SF_4$ + graphene

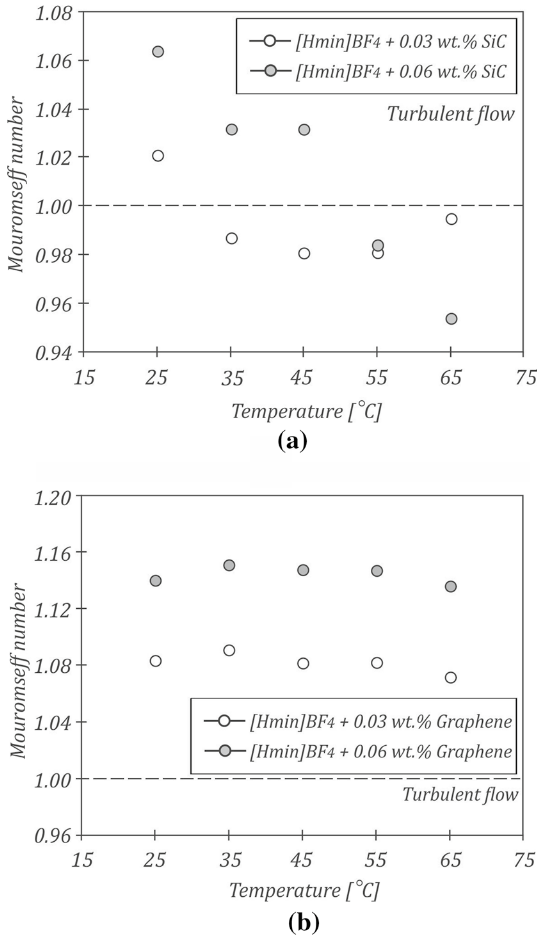

Fig. 5 Heat transfer efficiency based on Eq. 8

ionanofluid, it can be seen that the values of Mo number are higher than 1. Compared to $[H_{mim}]SF_4 + SiC$ ionanofluid, the values of Mo number are not affected by temperature, these being constant approximately with increasing temperature.

Another equation to evaluate of the heat transfer capability of fluids in internal turbulent flow is proposed by Vajiha and Das [19]:

$$FOM = \frac{Mo_{INF}}{Mo_{BF}} = \frac{\rho_{INF}^{0.8}}{\rho_{BF}^{0.8}} \frac{c_{p,INF}^{0.5}}{c_{p,BF}^{0.4}} \frac{k_{INF}^{0.5}}{k_{BF}^{0.6}} \frac{\mu_{BF}^{0.4}}{\mu_{INF}^{0.3}}. \quad (9)$$

Figure 6a, b illustrates the variation of figure-of-merit with temperature and concentration. The analysis made for the estimation of the heat transfer efficiency shows that the equation by Vajiha and Das [19] providing much higher results than the equation proposed by Mouromtseff [18]. Also, it can be noticed that the values of FOM slowly increase with increasing concentration, but decrease with

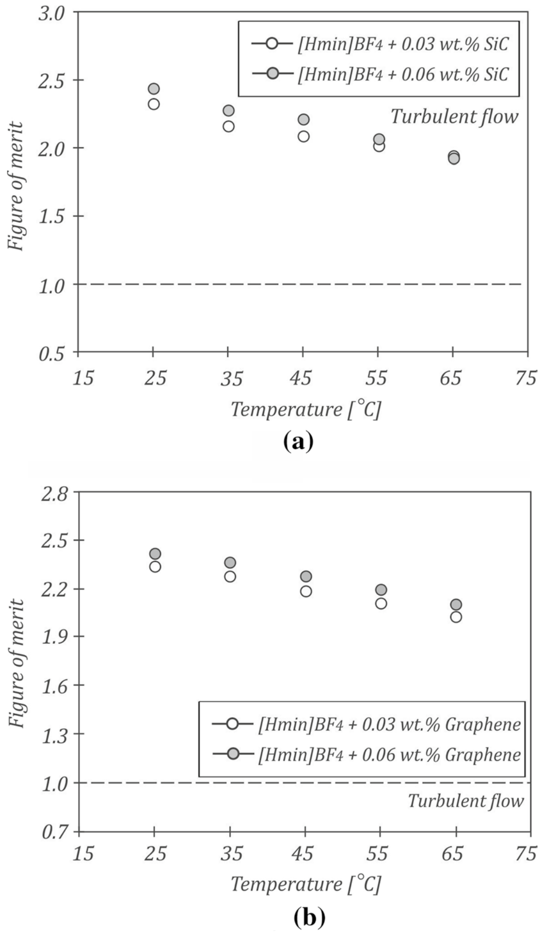

Fig. 6 Heat transfer efficiency based on Eq. 9

increasing temperature. Also, it can be noticed that the values of FOM for both studied ionanofluids computed with Eq. 9 are very close, slightly higher values being obtained in the case of $[H_{mim}]SF_4$ + graphene.

Tables 1 and 2 present the other results of the figure-of-merit computed on basis of Eqs. 10–21 [20] found in literature for forced single-phase convective heat transfer in turbulent flow.

- For cooling—the classical equation for the Fanning friction factor and the constant flow velocity:

Table 1 Figure-of-merit for $[H_{mim}]SF_4$ + SiC ionanofluids at various temperatures and concentrations in the turbulent flow

	Figure-of-merit								
	$[H_{mim}]$SF4 + SiC								
0.03 %					0.06 %				
25 °C	35 °C	45 °C	55 °C	65 °C	25 °C	35 °C	45 °C	55 °C	65 °C
	FOM_{T2}								
1.018	0.982	0.975	0.975	0.991	1.061	1.027	1.025	0.974	0.944
	FOM_{T3}								
0.981	0.941	0.926	0.931	0.950	0.987	0.945	0.941	0.873	0.848
	FOM_{T4}								
1.028	0.994	0.985	0.997	0.996	1.052	1.022	1.031	0.962	0.908
	FOM_{T5}								
1.028	0.998	0.995	0.995	1.005	1.072	1.047	1.048	1.007	0.976
	FOM_{T6}								
0.991	0.957	0.945	0.950	0.963	0.998	0.963	0.962	0.903	0.877
	FOM_{T7}								
1.038	1.01	1.005	1.017	1.010	1.063	1.042	1.054	0.995	0.939
	FOM_{T8}								
1.018	0.982	0.975	0.975	0.991	1.061	1.027	1.025	0.974	0.944
	FOM_{T9}								
0.978	0.934	0.918	0.921	0.942	0.983	0.937	0.932	0.859	0.834
	FOM_{T10}								
1.025	0.987	0.976	0.987	0.987	1.047	1.013	1.021	0.947	0.893
	FOM_{T11}								
1.028	0.998	0.995	0.995	1.005	1.072	1.047	1.048	1.007	0.976
	FOM_{T12}								
0.987	0.950	0.936	0.940	0.955	0.994	0.955	0.952	0.888	0.862
	FOM_{T13}								
1.035	1.003	0.996	1.007	1.001	1.059	1.033	1.043	0.979	0.923

Table 2 Figure-of-merit for $[H_{mim}]SF_4$ + graphene ionanofluids at various temperatures and concentrations in the turbulent flow

	Figure-of-merit ratio								
	$[H_{mim}]SF4$ + graphene								
0.03 %					0.06 %				
25 °C	35 °C	45 °C	55 °C	65 °C	25 °C	35 °C	45 °C	55 °C	65 °C
	FOM_{T2}								
1.091	1.098	1.087	1.088	1.077	1.151	1.162	1.159	1.158	1.146
	FOM_{T3}								
1.143	1.143	1.126	1.126	1.110	1.212	1.226	1.221	1.216	1.199
	FOM_{T4}								
1.116	1.127	1.108	1.107	1.093	1.184	1.201	1.194	1.188	1.171
	FOM_{T5}								
1.069	1.075	1.066	1.067	1.059	1.116	1.125	1.123	1.123	1.113
	FOM_{T6}								
1.110	1.119	1.104	1.104	1.091	1.175	1.188	1.183	1.178	1.164
	FOM_{T7}								
1.095	1.103	1.087	1.085	1.074	1.148	1.163	1.156	1.151	1.137
	FOM_{T8}								
1.091	1.098	1.087	1.088	1.077	1.151	1.162	1.159	1.158	1.146
	FOM_{T9}								
1.135	1.148	1.129	1.129	1.113	1.218	1.233	1.227	1.222	1.203
	FOM_{T10}								
1.120	1.132	1.111	1.110	1.096	1.190	1.208	1.200	1.193	1.175
	FOM_{T11}								
1.069	1.075	1.066	1.067	1.059	1.116	1.125	1.123	1.123	1.113
	FOM_{T12}								
1.113	1.124	1.108	1.108	1.094	1.181	1.194	1.189	1.184	1.169
	FOM_{T13}								
1.098	1.108	1.09	1.089	1.077	1.154	1.170	1.162	1.157	1.141

$$FOM_{T2} = \frac{Mo_{INF}}{Mo_{BF}} = \left(\frac{\rho_{INF}}{\rho_{BF}}\right)^{\frac{4}{5}} \left(\frac{c_{p,INF}}{c_{p,BF}}\right)^{\frac{3}{10}} \left(\frac{\mu_{INF}}{\mu_{BF}}\right)^{-\frac{1}{2}} \left(\frac{k_{INF}}{k_{BF}}\right)^{\frac{7}{10}}, \tag{10}$$

$$FOM_{T3} = \frac{h_{INF}/h_{BF}}{W_{INF}/W_{BF}} = \left(\frac{c_{p,INF}}{c_{p,BF}}\right)^{\frac{3}{10}} \left(\frac{\mu_{INF}}{\mu_{BF}}\right)^{-\frac{7}{10}} \left(\frac{k_{INF}}{k_{BF}}\right)^{\frac{7}{10}}, \tag{11}$$

$$FOM_{T4} = \frac{c_{p,INF}h_{INF}/W_{INF}}{c_{p,BF}h_{BF}/W_{BF}} = \left(\frac{c_{p,INF}}{c_{p,BF}}\right)^{\frac{13}{10}} \left(\frac{\mu_{INF}}{\mu_{BF}}\right)^{-\frac{7}{10}} \left(\frac{k_{INF}}{k_{BF}}\right)^{\frac{7}{10}}. \tag{12}$$

- For heating—the classical equation for the Fanning friction factor and the constant flow velocity:

$$FOM_{T5} = \frac{Mo_{INF}}{Mo_{BF}} = \left(\frac{\rho_{INF}}{\rho_{BF}}\right)^{\frac{4}{5}} \left(\frac{c_{p,INF}}{c_{p,BF}}\right)^{\frac{2}{5}} \left(\frac{\mu_{INF}}{\mu_{BF}}\right)^{-\frac{2}{5}} \left(\frac{k_{INF}}{k_{BF}}\right)^{\frac{3}{5}}, \tag{13}$$

$$FOM_{T6} = \frac{h_{INF}/h_{BF}}{W_{INF}/W_{BF}} = \left(\frac{c_{p,INF}}{c_{p,BF}}\right)^{\frac{2}{5}} \left(\frac{\mu_{INF}}{\mu_{BF}}\right)^{-\frac{3}{5}} \left(\frac{k_{INF}}{k_{BF}}\right)^{\frac{3}{5}}, \tag{14}$$

$$FOM_{T7} = \frac{c_{p,INF}h_{INF}/W_{INF}}{c_{p,BF}h_{BF}/W_{BF}} = \left(\frac{c_{p,INF}}{c_{p,BF}}\right)^{\frac{7}{5}} \left(\frac{\mu_{INF}}{\mu_{BF}}\right)^{-\frac{3}{5}} \left(\frac{k_{INF}}{k_{BF}}\right)^{\frac{3}{5}}. \tag{15}$$

- For cooling—the Blasius equation for the Fanning friction factor and the constant flow velocity:

$$FOM_{T8} = \frac{Mo_{INF}}{Mo_{BF}} = \left(\frac{\rho_{INF}}{\rho_{BF}}\right)^{\frac{4}{5}} \left(\frac{c_{p,INF}}{c_{p,BF}}\right)^{\frac{3}{10}} \left(\frac{\mu_{INF}}{\mu_{BF}}\right)^{-\frac{1}{2}} \left(\frac{k_{INF}}{k_{BF}}\right)^{\frac{7}{10}}, \tag{16}$$

$$FOM_{T9} = \frac{h_{INF}/h_{BF}}{W_{INF}/W_{BF}} = \left(\frac{\rho_{INF}}{\rho_{BF}}\right)^{\frac{1}{20}} \left(\frac{c_{p,INF}}{c_{p,BF}}\right)^{\frac{3}{10}} \left(\frac{\mu_{INF}}{\mu_{BF}}\right)^{-\frac{3}{4}} \left(\frac{k_{INF}}{k_{BF}}\right)^{\frac{7}{10}}, \tag{17}$$

$$FOM_{T10} = \frac{c_{p,INF}h_{INF}/W_{INF}}{c_{p,BF}h_{BF}/W_{BF}} = \left(\frac{\rho_{INF}}{\rho_{BF}}\right)^{\frac{1}{20}} \left(\frac{c_{p,INF}}{c_{p,BF}}\right)^{\frac{13}{10}} \left(\frac{\mu_{INF}}{\mu_{BF}}\right)^{-\frac{3}{4}} \left(\frac{k_{INF}}{k_{BF}}\right)^{\frac{7}{10}}. \tag{18}$$

- For heating—the Blasius equation for the Fanning friction factor and the constant flow velocity:

$$FOM_{T11} = \frac{Mo_{INF}}{Mo_{BF}} = \left(\frac{\rho_{INF}}{\rho_{BF}}\right)^{\frac{4}{5}} \left(\frac{c_{p,INF}}{c_{p,BF}}\right)^{\frac{2}{5}} \left(\frac{\mu_{INF}}{\mu_{BF}}\right)^{-\frac{2}{5}} \left(\frac{k_{INF}}{k_{BF}}\right)^{\frac{3}{5}}, \tag{19}$$

$$FOM_{T12} = \frac{h_{INF}/h_{BF}}{W_{INF}/W_{BF}} = \left(\frac{\rho_{INF}}{\rho_{BF}}\right)^{\frac{1}{20}} \left(\frac{c_{p,INF}}{c_{p,BF}}\right)^{\frac{2}{5}} \left(\frac{\mu_{INF}}{\mu_{BF}}\right)^{-\frac{13}{20}} \left(\frac{k_{INF}}{k_{BF}}\right)^{\frac{3}{5}}, \tag{20}$$

$$FOM_{T13} = \frac{c_{p,INF}h_{INF}/W_{INF}}{c_{p,BF}h_{BF}/W_{BF}} = \left(\frac{\rho_{INF}}{\rho_{BF}}\right)^{\frac{1}{20}} \left(\frac{c_{p,INF}}{c_{p,BF}}\right)^{\frac{7}{5}} \left(\frac{\mu_{INF}}{\mu_{BF}}\right)^{-\frac{13}{20}} \left(\frac{k_{INF}}{k_{BF}}\right)^{\frac{3}{5}}. \tag{21}$$

One can notice that the values of FOM for $[H_{mim}]SF_4$ + graphene are higher than 1 for all temperatures and concentrations, which indicate that this type of ionanofluids can be a good choice to be used in heat transfer applications. And in these cases, it can be seen that the FOM values computed with Eqs. 10–21 are lower than those calculated with Eq. 9 [19], the results being in accordance with the results obtained with Eq. 8 [18].

3.2 Pumping Power

In contrast to the Mouromtseff number, which is based on thermo-physical properties of ionanofluids, for the estimation of the pumping power only viscosity and density are needed. If the pumping power ratio is less than 1, then the ionanofluids can be useful for heat transfer applications.

In this regard, the pumping power for the laminar and turbulent flows was evaluated with following equations [21]:

– In laminar flow:

$$W_L = \frac{\mu_{INF}}{\mu_{BF}} \left(\frac{\rho_{BF}}{\rho_{INF}} \right)^2. \tag{22}$$

– In turbulent flow:

$$W_T = \left(\frac{\mu_{INF}}{\mu_{BF}} \right)^{0.25} \left(\frac{\rho_{BF}}{\rho_{INF}} \right)^2. \tag{23}$$

Figure 7a, b depicts the pumping power ratio for various temperatures and concentrations in the laminar flow. As can be seen, the pumping power ratio is higher than 1 for $[H_{mim}]SF_4$ + SiC ionanofluid, and lower than 1 for $[H_{mim}]SF_4$ + graphene ionanofluid in all the studied temperatures and concentrations. Moreover, for $[H_{mim}]SF_4$ + SiC ionanofluid it can be noticed that the pumping power ratio increases with increasing temperature, and also that adding nanoparticles in the base fluid influence the pumping power only at temperatures above 45 °C. Concerning the $[H_{mim}]SF_4$ + graphene ionanofluid, it can be stated that can be used in heat transfer applications, the minimum value of pumping power ratio being obtained at a temperature of 35 °C for both studied concentrations.

Figure 8a, b shows the pumping power ratio with the variation of both temperatures and concentrations in the turbulent flow. Compared to the laminar flow, the $[H_{mim}]SF_4$ + SiC ionanofluid with a concentration of 0.06 % and temperatures up to 55 °C can be used in thermal applications, while $[H_{mim}]SF_4$ + graphene ionanofluid cannot be recommended for heat transfer applications, since the values of pumping power ratio for all temperatures and concentrations is higher than 1.

Finally, to have a complete image on heat transfer efficiency of studied ionanofluids, the results discussed above are summarized in Table 3.

Fig. 7 Pumping power ratio in laminar flow

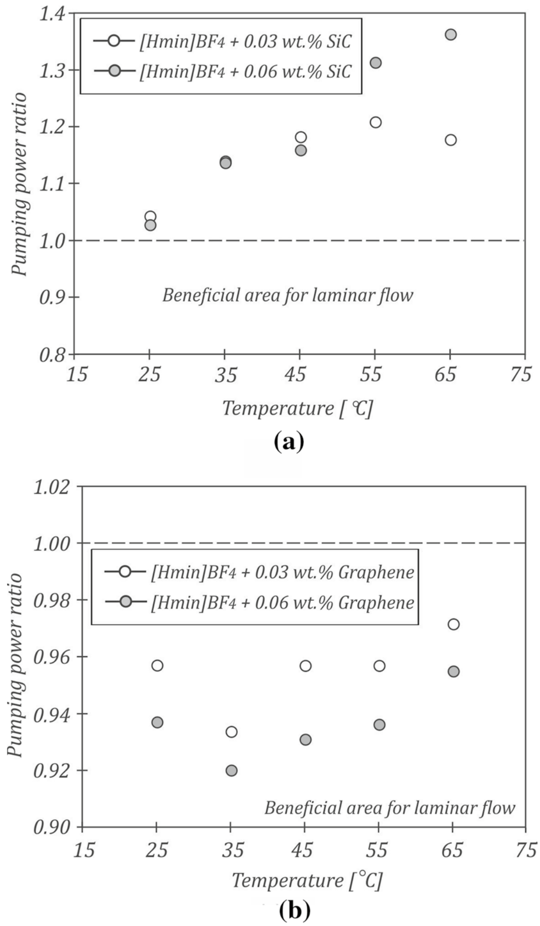

4 Conclusions

In this paper, heat transfer efficiency of ionanofluids in laminar and turbulent flows was investigated. The comprehensive analysis was based on the experimental data of $[H_{mim}]SF_4$ + SiC and $[H_{mim}]SF_4$ + graphene ionanofluids (thermal conductivity, dynamic viscosity, specific heat and density). The conclusions of this study are:

- In laminar flow, both studied ionanofluids have a higher efficiency than the base fluid ($[H_{mim}]SF_4$);
- In turbulent flow, $[H_{mim}]SF_4$ + graphene ionanofluid is beneficial for heat transfer applications at all studied temperatures and concentrations.

Fig. 8 Pumping power ratio in turbulent flow

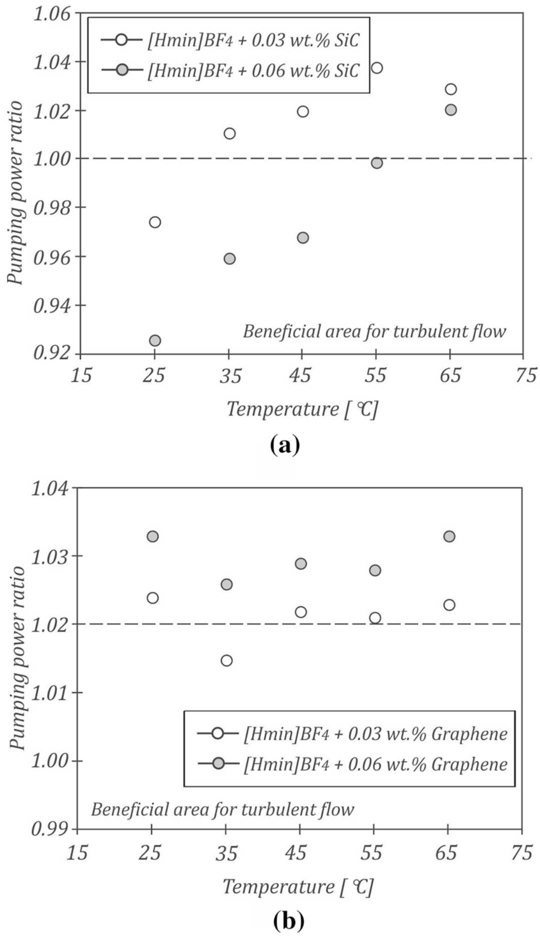

- In laminar flow, the values of the pumping power ratio are higher than 1 for $[H_{mim}]SF_4$ + SiC ionanofluid, and lower than 1 for $[H_{mim}]SF_4$ + graphene ionanofluid at all studied temperatures and concentrations, which indicate that $[H_{mim}]SF_4$ + graphene ionanofluid can be used in heat transfer applications;
- In turbulent flow, the values of the pumping power ratio indicated that using the ionanofluids leads to a penalty in pumping power.

Table 3 Heat transfer efficiency of studied ionanofluids

$[H_{mim}]SF4+SiC$						$[H_{mim}]SF4+graphene$					
Laminar flow			Turbulent flow			Laminar flow			Turbulent flow		
$C_\mu/C_k < 4$	$Mo > 1$	$W_L < 1$	$Mo > 1$	$FOM > 1$	$W_T < 1$	$C_\mu/C_k < 4$	$Mo > 1$	$W_L < 1$	$Mo > 1$	$FOM > 1$	$W_T < 1$
Good	Good	Weak	Only the 0.06 % concentration with temperatures up to 45 °C	Good	Only the 0.06 % concentration with temperatures up to 55 °C	Good	Good	Good	Good	Good	Weak

References

1. A.P.C. Ribeiro, M.J.V. Lourenço, C.A.N. de Castro, in *17th Symp. Thermophys. Prop.* Boulder, USA, (2009).
2. F.F. Zhang, F.F. Zheng, X.H. Wu, Y.L. Yin, G. Chen, R. Soc, Open Sci. **6**, 182040 (2019)
3. T.C. Paul, A.K.M.M. Morshed, E.B. Fox, J.A. Khan, Appl. Therm. Eng. **110**, 1–9 (2017)
4. S. Jorjani, M. Mozaffarian, G. Pazuki, J. Mol. Liq. **271**, 211–219 (2018)
5. E.I. Cherecheş, J.I. Prado, C. Ibanescu, M. Danu, A.A. Minea, L. Lugo, J. Mol. Liq. **317**, 114020 (2020)
6. E.I. Chereches, A.A. Minea, K.V. Sharma, Int. J. Heat Mass Transf. **154**, 119674 (2020)
7. E.I. Cherecheş, A.A. Minea, J. Therm. Anal. Calorim. (In press). https://doi.org/https://doi.org/10.1007/s10973-020-09925-z
8. H. Xie, Z. Zhao, J. Zhao, H. Gao, Chinese J Chem. Eng. **24**, 331–338 (2016)
9. L. Zhang, L. Chen, J. Liu, X. Fang, Z. Zhang, Renew. Energ. **99**, 888–897 (2016)
10. A.A. Minea, Int. J. Thermophys **41**, 151–166 (2020)
11. A.A. Minea, S.M.S. Murshed, Renew. Sust. Energy Rev. **91**, 584–599 (2018)
12. S. Wegner, C. Janiak, Top. Curr. Chem. (Z) **375**, 65–87 (2017)
13. B. Bakthavatchalam, K. Habib, R. Saidur, B.B. Saha, K. Irshad, J. Mol. Liq. **305**, 112787 (2020)
14. W. Chen, C. Zou, X. Li, Sol. Energy Mater. Sol. C. **163**, 157–163 (2017)
15. J. Liu, F. Wang, L. Zhang, X. Fang, Z. Zhang, Renew. Energy **63**, 519–523 (2014)
16. R.E. Simons, Electronic Cool. **12** (2006)
17. R. Prasher, D. Song, J. Wang, P. Phelan, Appl. Phys. Lett. **89**, 133108 (2006)
18. I. Mouromtseff, Proc. IRE **30**, 190–205 (1942)
19. R.S. Vajjha, D.K. Das, Int. J. Heat Mass Transf. **55**, 4063–4078 (2012)
20. W. Yu, D.M. France, E.V. Timofeeva, D. Singh, J.L. Routbort, Int. J. Heat Mass Transf. **55**, 5380–5396 (2012)
21. R.B. Mansour, N. Galanis, C.T. Nguyen, Appl. Therm. Eng. **27**, 240–249 (2007)